Nonlinear Faraday rotation and detection of superposition states in cold atoms

Adam Wojciechowski,[1,2] Eric Corsini,[3,2] Jerzy Zachorowski,[1,2] and Wojciech Gawlik[1,2]
[1]*Institute of Physics, Jagiellonian University, Reymonta 4, PL-30-059 Kraków, Poland*
[2]*Joint Krakow-Berkeley Atomic Physics and Photonics Laboratory, Reymonta 4, PL-30-059 Kraków, Poland*
[3]*Department of Physics, University of California, Berkeley, California 94720-7300, USA*
(Received 15 December 2009; revised manuscript received 19 April 2010; published 24 May 2010)

We report on the observation of nonlinear Faraday rotation with cold atoms at a temperature of ~100 μK. The observed nonlinear rotation of the light polarization plane is up to 0.1 rad over the 1-mm-size atomic cloud in approximately 10-mG magnetic field. The nonlinearity of rotation results from long-lived coherence of ground-state Zeeman sublevels created by a near-resonant light. The method allows for creation, detection, and control of atomic superposition states. It also allows applications for precision magnetometry with high spatial and temporal resolution.

DOI: 10.1103/PhysRevA.81.053420 PACS number(s): 33.57.+c, 32.80.Xx, 42.50.Dv, 42.50.Gy

I. INTRODUCTION

The linear Faraday rotation (LFR) of the polarization plane of light propagating in the medium is a well-known consequence of optical anisotropy caused by a longitudinal magnetic field. For thermal gases the Doppler effect broadens the range of the magnetic fields where the effect is visible and reduces the size of the maximum rotation relative to atoms at rest. The use of cold atoms with their Doppler width narrower than the natural linewidth distinguishes this situation from experiments at room temperature. The experiments on LFR with cold atoms were performed in a magneto-optical trap (MOT) [1–3], and in an optical dipole trap [4].

Application of strong, near-resonant laser light may result in the creation of coherent superpositions of Zeeman sublevels of an atomic ground state. Such superpositions (Zeeman coherences) result in nonlinear optical properties of atomic sample and are known to be responsible for a variety of coherent phenomena in light-matter interaction. The most important examples are coherent population trapping [5], electromagnetically induced transparency [6], nonlinear magneto-optical rotation or nonlinear Faraday rotation (NFR) [7] and their interplay [8]. Superposition states are also at the heart of quantum-state engineering (QSE). Most of the QSE experiments require initial states of well-defined atomic spin (or total angular momentum F), usually prepared in a stretched state, which is realized by putting most of (ideally all) atomic population into a Zeeman sublevel with extreme value of magnetic quantum number m [9]. Below we report how superpositions of specific Zeeman sublevels, or Zeeman coherences belonging to a given F and corresponding to an aligned state are created in cold (~100 μK) atomic samples and observed with high sensitivity using nonlinear Faraday rotation. In the experiment, laser light both creates and detects the Zeeman coherences. The same detection technique can be applied to detect the presence of Zeeman coherences already introduced with other mechanisms, for example, in a pump-probe experiment. Furthermore, the time-dependent detection provides information on the temporal evolution of the superposition states.

The described experiment shows the potential of NFR with cold atoms for precision magnetometry with important prospective features: μG sensitivity, large dynamic range (zero-field to several G), and sub-mm spatial resolution in magnetic field mapping. Magnetic field sensing with cold atoms utilizing Larmor precession of alkali-metal atoms in a magnetic field has been discussed in: MOT [10], Bose-Einstein condensate [11,12], and an optical dipole trap [13]. Our measurements apply a different principle: Rather than measuring Larmor frequency we measure rotation of a polarization plane, which is more practical for very weak (near-zero) fields. In our experiment the rotation is mainly caused by the nonlinear medium's birefringence resulting from the light-induced Zeeman coherences [14,15], regarded as the diamagnetic effect. The rotation resulting from population imbalance (paramagnetic effect) was studied with cold atoms in recent experiments devoted to spin squeezing [16].

II. THEORETICAL BACKGROUND

For resonant excitation, rotation angle θ is a measure of circular birefringence, $\theta \propto n_+ - n_-$, where $n_\pm$ are the refractive indices for $\sigma^\pm$ polarized light and

$$n_\pm - 1 \propto \mathcal{E}^{-1} \sum_{eg} \mathrm{Re}(d_{eg}^{(\pm)} \rho_{eg}^{(\pm)}), \tag{1}$$

with $\mathcal{E}$ being the light electric field amplitude, $d_{eg}^{\pm}$ the matrix element of the dipole moment associated with the $\sigma^\pm$-polarized light-beam components, and $\rho_{eg}^{\pm}$ the related density matrix elements. The summation goes over all ground- and excited-state sublevels g and e linked by the allowed transitions, as shown in Fig. 1(b). In the stationary regime, ρ_{eg} can be expressed as

$$\rho_{eg}^{(\pm)} = \frac{1}{\delta_{eg} - i\Gamma/2} \sum_{e'g'} (\Omega_{eg'}^{(\pm)} \rho_{g'g} - \rho_{ee'} \Omega_{e'g}^{(\pm)}), \tag{2}$$

where $\delta_{\alpha\beta}$ and $\Omega_{\alpha\beta}$ denote, respectively, the light detuning and Rabi frequency for the $\alpha \leftrightarrow \beta$ transition, and $\Gamma/2$ is the relaxation rate of the optical coherence. The polarization index $\pm$ is related with magnetic quantum numbers of states e, g by standard selection rules for polarized light. Relations (1), (2) indicate that optical coherences, and consequently also the refractive indices and rotation angle, depend on the density matrix elements $\rho_{g'g}$ and $\rho_{ee'}$ which represent populations of and coherences between Zeeman sublevels of the ground and excited states. All couplings shown in Fig. 1(b) form

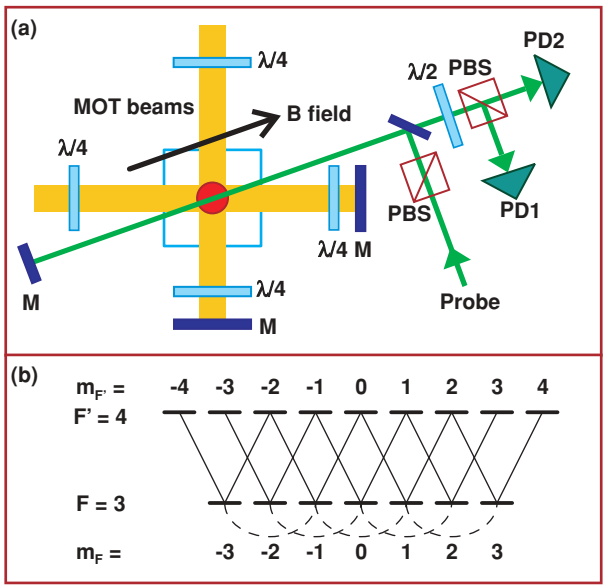

FIG. 1. (Color online) (a) The setup of the experiment for the balanced polarimeter arrangement. M, mirrors; PBS, polarizing beam splitters; PD, photodetectors; $\lambda/2$, $\lambda/4$, wave plates. Direction of the magnetic field B necessary for the observation of the Faraday rotation is indicated. (For FS scheme the $\lambda/2$ plate is removed and PD2 is not used). (b) Energy level structure with the Zeeman coherences established by a linearly polarized light resonant with the $F = 3 \rightarrow F' = 4$ transition.

independent generic Λ and V systems which involve coherences between ground- and excited-state sublevels, respectively, with $\Delta m = \pm 2$. For not-too-strong light, the excited-state coherences are negligible and the rotation signal becomes sensitive mainly to the ground-state coherences.

The main difficulty in observation of NFR with cold atoms is that at light intensity required for creation of the Zeeman coherence the laser beam may mechanically perturb the cold-atom sample. In our study this adverse effect is reduced by retroreflection of the light beam and careful optimization of the experimental conditions to minimize the light power.

III. EXPERIMENTAL SETUP

The experiment [(see the setup shown in Fig. 1(a)] was performed with about 10^7 ^{85}Rb atoms using a standard MOT. In addition to the trapping and repumping lasers we used a separate probe laser whose frequency was tuned around the $F = 3 \rightarrow F' = 4$ hyperfine transition of the D2 line (780 nm). Figure 1(b) depicts the Zeeman structure of the $F = 3$ and $F' = 4$ states with the transitions induced by linearly polarized light (superposition of $\sigma^{\pm}$ polarizations). A weak linearly polarized probe beam of several μW in power and 2 mm in diameter was sent through the atom cloud and retroreflected to partially reduce light pressure effects. This was possible due to low absorption, corresponding to resonant optical density OD ~ 0.5. The probe-beam frequency set 14 MHz below the line center proved to be optimal from the point of view of atomic loss which we attribute to extra Doppler-cooling mechanism by two counter-propagating beams. The double passage of light through the sample doubled the acquired Faraday rotation. The light polarization was measured in two configurations: using balanced polarimeter (direct rotation angle measurement) and in a crossed polarizers or forward-scattering (FS) scheme which for resonant light is sensitive to the square of the rotation angle. For the nonresonant case, circular dichroism contributes also to the observed signal.

In the experiment, atoms were collected and cooled in the MOT. This phase was periodically interrupted for the measurement of optical rotation: The trapping laser and the quadrupole magnetic field were switched off and a homogenous magnetic field B of a controlled value was applied along the probe beam. After 2 ms (required for complete decay of the eddy currents induced by turning off the quadrupole field), the probe beam was switched on and polarization rotation was recorded for the next 5 ms. Finally, the MOT fields were switched back for 50–200 ms and the atomic cloud was recaptured and cooled. During all measurements, the repumping laser was kept constantly on to avoid hyperfine pumping by the probing beam. This procedure allowed recording polarization rotation signals as a function of time for each value of the B field. The experiment was controlled by a PC, which also digitized, stored, and averaged (typically 20 times) the data.

IV. RESULTS

A. Unmodulated light; $B \sim 0$

Typical signals (rotation angle versus B) associated with linear and nonlinear Faraday effect at a given time have the form of dispersive resonances nested at $B = 0$, as shown in Fig. 2. The narrow feature is the nonlinear resonance (NFR); it appears when the probe beam is sufficiently intense. Hereinafter, we refer to this nonlinear resonance as the zero-field NFR resonance. The width of the linear resonance amounts to several G and corresponds to the natural linewidth of the studied transition. It also depends on the detuning of the probe beam from resonance condition and initial Zeeman-sublevel populations, as has been shown in [2]. That situation is prominently different from the case of vapor cells, where LFR resonance is two orders of magnitude broader, because of the Doppler effect.

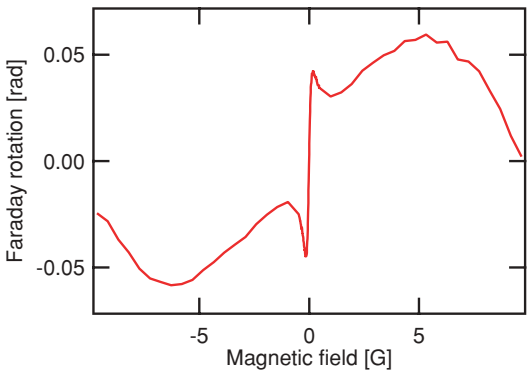

FIG. 2. (Color online) Linear (wide) and nonlinear (narrow) Faraday rotation resonances centered at $B = 0$. Signals were recorded at the time $\tau = 2$ ms after switching on the probing beam. The probe power is 64 μW. At that power the NFR resonance is substantially power broadened but is well visible in comparison with the LFR. The slope of the central part is $\approx$0,6 rad/G.

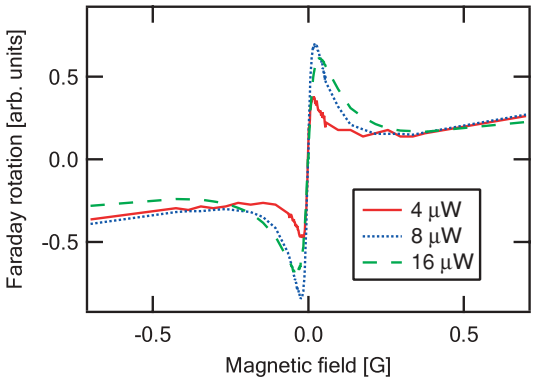

FIG. 3. (Color online) Evolution of the Faraday rotation with increasing light intensity of the probe beam showing the nonlinear increase and power broadening of the central resonance.

In Fig. 3 we depict the evolution of the Faraday rotation signals as a function of light power. While the wide structure associated with the linear Faraday effect represent rotation angle independent on the light intensity, the central narrow feature clearly exhibits nonlinear behavior. The narrow part is due to the superpositions of the ground-state Zeeman sublevels which differ by $|\Delta m| = 2$, shown in Fig. 1(b). These are thus the light-induced Zeeman coherences that are responsible for nonlinearity of the Faraday effect observed with appropriately strong light in very small magnetic fields. The narrow width results from the long lifetime of the ground-state superpositions which is a necessary prerequisite for qubits and QSE applications. In case of atoms released from the MOT, the main mechanism of the resonance broadening is the escape time of atoms from the observation volume due to gravitation and their initial momenta. There is also light-induced expelling of atoms from the probed volume which is responsible for the drop of maximal rotation seen in Fig. 3 as probe power is increased from 8 to 16 μW. The atom number reduction can also be independently measured by monitoring the total intensity of the transmitted probe beam. Another major contribution to the finite resonance width comes from transverse magnetic fields, and can be understood as power broadening due to magnetically driven transitions between degenerate Zeeman sublevels for the near-zero fields. Therefore, dc and low-frequency transverse magnetic field components have to be precisely compensated for the NFR observation. Other broadening mechanisms include gradient of the longitudinal magnetic field and power broadening due to the probing beam. The latter can be reduced by using appropriate intensity and detuning. Moreover, and as pointed out in Sec. III, red detuning of the retroreflected probe beam reduces the atom loss. This indicates that there is an extra cooling effect by spontaneous light forces associated with the probe beam.

By compensation of the transverse fields the minimum width of the zero-field resonance was achieved; in our setup it was about 10 mG. This is significantly more than the values which are available with the state-of-art paraffine-coated glass cells in magnetically shielded environments where typical widths are of the order of 1 μG, yet the central part of the NFR resonance has a slope of up to 10 rad/G that would correspond to a Verdet constant of 10^8 rad/T m. We attribute

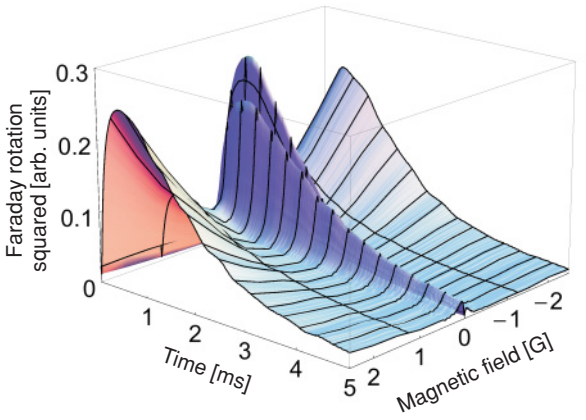

FIG. 4. (Color online) Time evolution of linear (wide) and nonlinear (narrow) Faraday rotation resonances in FS arrangement where the signal is proportional to magneto-optical rotation angle squared. Probe power is 18 μW.

the larger width to the finite interaction time of the cold atom cloud and to the magnetic-field inhomogeneities in our unshielded experimental setup. The two mechanisms could be significantly reduced by application of an optical dipole trap. Such traps allow longer interaction times and allow one to work with more confined atom samples where field inhomogeneities are less important.

Time evolution of Faraday rotation squared (FS arrangement) is depicted in Fig. 4. The linear effect (signal seen at the wings corresponding to strong magnetic fields) depends only on number of atoms and Zeeman population distribution and thus follows the temporal evolution of these quantities. The nonlinear effect (seen in a narrow magnetic-field range around $B = 0$) results from light-atom interaction (i.e., optical pumping with linearly polarized light) and thus requires some, light-intensity-dependent, time to build up. This effect is well illustrated in Fig. 5, where examples of such evolution for two different light intensities are presented. Unlike the linear contribution, the onset of which is limited only by the detector time constant, the initial slopes of the nonlinear contributions indeed depend on the probe power. The coherence buildup times appear longer than the optical pumping times necessary

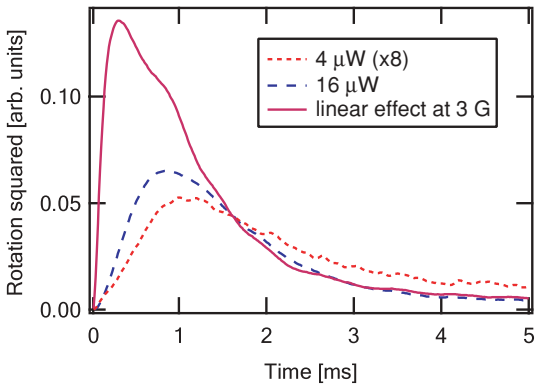

FIG. 5. (Color online) Time dependence of the nonlinear Faraday rotation with a 45-mG magnetic field at two different probe beam powers (4 μW, magnified eight times, and 16 μW) compared to the time dependence of the linear Faraday rotation at 3 G and 16 μW.

for population redistribution corresponding to the applied light intensities. This is the consequence of the fact that atomic coherences, in contrast to atomic populations, are very sensitive to various dephasing processes. For Zeeman coherences (i.e., superpositions of the magnetic sublevels), it is the magnetic-field inhomogeneity (spatial and temporal) which generates the strongest dephasing. Such dephasing makes it necessary to use higher light intensities and/or longer interaction times for creation and detection of coherences than mere population redistribution.

Both signals in Fig. 5 decay as atoms escape from the probed volume. The separation between the linear and nonlinear contributions corresponding to a given light power is done based on the magnetic field strength: At about 45 mG the LFR is negligible and NFR dominates the rotation, whereas the opposite is true for magnetic fields of 3 G and above. The signal decay constant appears to be slower for lower light intensity while for constant intensity it is the same for NFR at 45 mG and for LFR at 3 G. Additionally, the decaying slopes of the LFR and NFR signals recorded for the same light intensity do not differ much. These observations prove that the light-pressure expelling of atoms from the observation volume is the main mechanism of signal decay.

B. Amplitude modulated light; $B \neq 0$

Stationary ground-state coherences are destroyed when the Larmor precession becomes faster than the coherence relaxation time, which limits direct observation of the NFR signals to a narrow range (some mG) around $B = 0$. One possibility to observe NFR not only around the zero magnetic field is to use modulation techniques. Two arrangements have been proposed using either frequency (FM NMOR [17]) or amplitude (AMOR [18]) modulation of light. In both arrangements strobed pumping creates the modulated Zeeman coherence and phase sensitive detection is used to extract the magneto-optical rotation amplitude. In addition to the zero-field resonance, two other resonances appear in the demodulated rotation signal when the modulation frequency Ω_m meets $\pm$ twice Larmor precession frequency in a given magnetic field. These high-field resonances result from the optical pumping synchronous with the Larmor precession. The factor of 2 appears because the twofold symmetry of the optical anisotropy associated with $|\Delta m| = 2$ coherences yields modulation at precisely twice the Larmor precession. The width of these resonances is determined by the coherence lifetime and, in case of long-lived ground states, can be as narrow as the zero-field resonance.

In our experiment, the AMOR technique was applied: The probe beam was periodically chopped using the acousto-optical modulators. Use of modulation frequencies up to $\sim$10 MHz allowed detection of resonances in magnetic fields as large as 10 G. This is an order of magnitude higher field compared to previous FM NMOR and AMOR work and demonstrates the method's potential for precision magnetometry in a wide range of fields. This range can be further extended by using electro-optical modulators up to the fields where Zeeman coherences might be deteriorated by the Back-Goudsmit effect. Figure 6 shows NFR signal with two AMOR resonances at $\pm$3 G that are the evidence of driving $|\Delta m| = 2$ coherences at nonzero magnetic fields. This signal

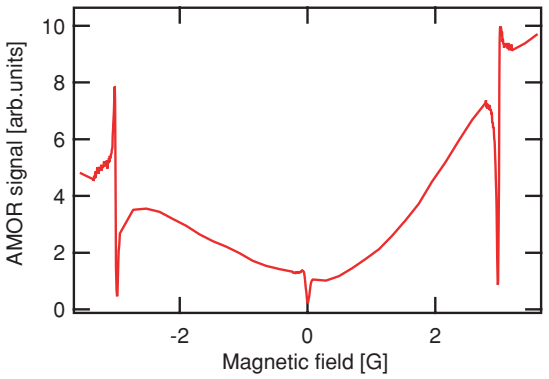

FIG. 6. (Color online) NFR with amplitude modulated light (AMOR). The narrow central resonance is a typical NFR zero-field resonance and the two high field resonances at $\pm$3 G result from amplitude modulation of the light with $\Omega_m = 2.8$ MHz.

was recorded with the FS configuration, hence it is symmetric around $B = 0$. The broad background is the LFR and the slight asymmetry of resonance shapes can be attributed to experimental setup imperfection.

V. SUMMARY AND CONCLUSIONS

The nonlinear Faraday rotation in a sample of cold atoms has been studied both with unmodulated and modulated laser beams. The use of retroreflected beam alleviated the problem of mechanical perturbation of the cold atoms by the probe beam and allowed studies of nonlinear magneto-optical effects in cold trapped atoms. In contrast to previous experiments with pure quantum states of oriented spins, the NFR measurements allow control and convenient studies of long-lived superposition states of aligned spins (i.e., quantum superpositions of Zeeman sublevels belonging to a given F). In particular, we were able to vary the degree of Zeeman coherence and monitor its buildup and decay, both in the stationary regime ($B \simeq 0$), and for Larmor frequencies up to 10 MHz. The relatively long buildup time of the NFR signals revealed the different dynamics governing ground state coherences and atomic populations. In addition to its potential for QSE, the NFR effect can be used for measuring a wide range of transient and static magnetic fields with 10-μs time resolution, sub-mG sensitivity, and mm spatial resolution given by the size of the cold atom cloud or the beam waist size. The current results are limited mostly by finite lifetime of trapped atoms and power broadening by the probe beam. Transfer of atoms into an optical dipole trap would make probing time much longer ($\sim$1 s) and the light-atom coupling more effective whereas the use of separate pump and probe beams as opposed to a single pump-probe beam would alleviate power broadening limitations.

ACKNOWLEDGMENTS

The authors acknowledge valuable discussions with D. Budker, W. Chalupczak, R. Kaiser, M. Kubasik, and S. Pustelny. This work has been supported by the Polish Ministry of Science (Grant No. N N505 092033 and N N202 046337), the Foundation for Polish Science Team Program, and the National Science Foundation Global Scientists Program.

[1] S. Franke-Arnold, M. Arndt, and A. Zeilinger, J. Phys. B **34**, 2527 (2001).
[2] G. Labeyrie, C. Miniatura, and R. Kaiser, Phys. Rev. A **64**, 033402 (2001).
[3] J. Nash and F. A. Narducci, J. Mod. Opt. **50**, 2667 (2003).
[4] M. L. Terraciano, M. Bashkansky, and F. K. Fatemi, Phys. Rev. A **77**, 063417 (2008).
[5] E. Arimondo, in *Progress in Optics*, edited by E. Wolf (Elsevier, Amsterdam, 1996), Vol. 35, pp. 259–354.
[6] M. Fleischhauer, A. Imamoglu, and J. P. Marangos, Rev. Mod. Phys. **77**, 633 (2005).
[7] D. Budker, W. Gawlik, D. F. Kimball, S. M. Rochester, V. V. Yashchuk, and A. Weis, Rev. Mod. Phys. **74**, 1153 (2002).
[8] R. Drampyan, S. Pustelny, and W. Gawlik, Phys. Rev. A **80**, 033815 (2009).
[9] B. Julsgaard, J. Sherson, J. L. Sørensen, and E. S. Polzik, J. Opt. B: Quantum Semiclass. Opt. **6**, 5 (2004).
[10] T. Isayama, Y. Takahashi, N. Tanaka, K. Toyoda, K. Ishikawa, and T. Yabuzaki, Phys. Rev. A **59**, 4836 (1999).
[11] S. Wildermuth, S. Hofferberth, I. Lesanovsky, S. Groth, P. Krüger, J. Schmiedmayer, and I. Bar-Joseph, Appl. Phys. Lett. **88**, 264103 (2006).
[12] M. Vengalattore, J. M. Higbie, S. R. Leslie, J. Guzman, L. E. Sadler, and D. M. Stamper-Kurn, Phys. Rev. Lett. **98**, 200801 (2007).
[13] M. L. Terraciano, M. Bashkansky, and F. K. Fatemi, Opt. Express **16**, 13062 (2008).
[14] G. W. Series, Proc. Phys. Soc. **88**, 995 (1966).
[15] C. Cohen-Tannoudji and F. Laloë, J. Phys. (Paris) **28**, 505 (1967); **28**, 722 (1967).
[16] M. Kubasik, M. Koschorreck, M. Napolitano, S. R. de Echaniz, H. Crepaz, J. Eschner, E. S. Polzik, and M. W. Mitchell, Phys. Rev. A **79**, 043815 (2009).
[17] D. Budker, D. F. Kimball, V. V. Yashchuk, and M. Zolotorev, Phys. Rev. A **65**, 055403 (2002).
[18] W. Gawlik, L. Krzemień, S. Pustelny, D. Sangla, J. Zachorowski, M. Graf, A. O. Sushkov, and D. Budker, Appl. Phys. Lett. **88**, 131108 (2006).